

# Hydrogen evolution and oxidation—a prototype for an electrocatalytic reaction

E. Santos · A. Lundin · K. Pötting ·  
P. Quaino · W. Schmickler

Received: 12 August 2008 / Revised: 1 October 2008 / Accepted: 6 October 2008 / Published online: 31 October 2008  
© Springer-Verlag 2008

**Abstract** Due to progress in the theory of electrocatalysis and in quantum chemistry, it has become possible to investigate the hydrogen reaction and perform quantitative calculations for the reaction rate. First, we demonstrate this with model calculations for the adsorption of hydrogen on Pt(111). In accordance with experimental data, we find hydrogen adsorption at a potential above the equilibrium potential and with an almost vanishing energy of activation. As a second example, we explain trends in the catalytic activity of palladium overlayers and clusters on Au(111) electrodes.

## Introduction

An overly obsession with hydrogen evolution has delayed the development of electrochemistry by at least a decade—J. O'M. Bockris.

Unfortunately, the hydrogen electrode must be considered to be an extremely complicated

example. This may well be the reason for the relatively slow development of electrode kinetics—K. J. Vetter

For everything there is a season, and a time to every purpose under the heavens—Ecclesiastes 3:1.

It is easy to see why hydrogen is so fascinating: It is the lightest element of all, the most abundant element in the universe, and the main constituent of stars; on earth, electrochemistry offers the most convenient method for the generation of hydrogen, and also for its consumption as a fuel. Also, it is a prime example for electrocatalysis: The rates of hydrogen evolution and reduction vary by more than six orders of magnitude on the various metals. Put into everyday terms, on *sp* metals like mercury and cadmium, this reaction proceeds with the speed of an ant crawling on a leaf; on some transition metals, like platinum, it proceeds with the speed of a supersonic jet. Unfortunately, the prices of the metals follow their catalytic effectivity, and if mercury can be bought for the price of a scooter, platinum costs as much as a Ferrari race car.

Both the Tafel equation [1] and the more general Butler–Volmer law [2] have been originally developed for the hydrogen electrode. Subsequently, much effort was spent to understand the dependence of the reaction rate on the electrode material to understand the nature of hydrogen electrocatalysis. By necessity, much of this early work was phenomenological, and correlations were established between the reaction rate and various properties such as the work function [3], the strength of the metal–oxygen bond [4, 5], and the presence of unfilled *d*-orbitals [6]. All these attempts had limited success and contributed little to our understanding of

---

Dedicated to J.O'M. Bockris on the occasion of his 85th birthday and in recognition of his contributions to electrochemistry.

---

E. Santos  
Facultad de Matemática, Astronomía y Física,  
IFFaMAF-CONICET Universidad Nacional de Córdoba,  
Córdoba, Argentina

E. Santos · A. Lundin · K. Pötting ·  
P. Quaino · W. Schmickler (✉)  
Institute of Theoretical Chemistry,  
University of Ulm, 89069 Ulm, Germany  
e-mail: wolfgang.schmickler@uni-ulm.de

electrocatalysis. It was clear that *d* bands were important because all good catalysts, such as platinum and palladium, are *d* metals. However, on other *d* metals, such as nickel and cobalt, the reaction proceeds quite slowly, and so the mere presence of a *d* band is not sufficient to assure good catalytic properties.

The first theories of reactions relevant to electrochemistry were those of Marcus [7], Hush [8], and Levich and Dogonadze [9]. Although these theories consider only outer-sphere electron transfer, they were immediately applied to the hydrogen reaction—a futile attempt, as has been repeatedly pointed out by J. O'M. Bockris. We will come back to these theories below because they do contain a concept that is also of great importance to the Volmer reaction  $H^+ + e^- \rightarrow H_{ad}$ , namely, the energy of reorganization of the solvent.

With hindsight, it is easy to see that the tools required for understanding electrocatalysis were missing until recently. Up to the early 1990s, quantum chemical calculations were limited to small molecules, and the available theories lacked a detailed description of the interaction between the reactant and the electrode. All this has changed in the last few years, so now is the time and the season to investigate the hydrogen reaction!

### Tools to investigate electrocatalysis

During the last few decades, the development of programs based on density functional theory (DFT) has led to spectacular advances in quantum chemistry, in particular in its application to surfaces. With available packages, the structures of metal surfaces, bare or covered by adsorbates, can be calculated routinely. For reactions that do not involve the formation of ions, such as those that proceed in ultrahigh vacuum, even the reaction paths and the energies of activation can be determined. Although DFT contains a semiempirical element, because the exact form of the exchange and correlation functional is not known, the various approximations based on the generalized gradient approximation and on pseudopotentials that describe the core electrons generally give good results for the ground states, and the relative error in the energies between similar structures is usually of the order of 0.1 eV. Although a few spectacular failures of DFT are known, the large body of results obtained gives a good guidance on which variant gives good results under certain circumstances.

With DFT, it is possible to calculate the adsorption energy of hydrogen on single-crystal surfaces, and in order to mimic the electrochemical interface, it is even possible to include some water and an electric field

in the system [5, 27]. Also, purely chemical reaction steps like the recombination of two adsorbed hydrogen atoms to form the molecule can be described by DFT, but charge transfer steps, like the Volmer reaction  $H^+ + e^- \rightarrow H_{ad}$ , cannot. Charge transfer depends on the double layer structure, and the interaction of the ions with water is most important, since it is the hydration shell that stabilizes the ions. Indeed, the proton is an extreme case, since it has the highest hydration energy of all particles, of the order of 11 eV. Therefore, realistic calculations for the Volmer reaction would require an extremely large ensemble size that is well beyond the limits of present-day computers. Nevertheless, a few attempts have been made in this direction [10–12]; although these large-scale calculations do provide some interesting details, they all suffer from the fact that the ensembles are too small to represent the double layer and that the electrode potential is ill defined.

In our own approach to electrocatalysis, we use DFT only as a means to obtain system parameters, while the theory itself is based on a Hamiltonian devised by Santos, Koper, and Schmickler [14, 15]. In spirit, this model follows the older theories of outer-sphere electron transfer, but it gives a detailed description for the interaction between the reactant and the electronic bands of the metal and provides a mechanism for bond breaking. More than this, it explains how a metal can catalyze electron transfer through a strong interaction with a *d* band situated near the Fermi level [16, 17]. Just like in the Marcus theory, the inclusion of the electrode potential, which shifts the energy levels, is no principal problem, and the interaction with the solvent is incorporated through the energy of reorganization. However, in order to perform calculations for specific systems, we require DFT to obtain the band structure of metals and the interaction of the reactant with these bands. In the following sections, we shall illustrate how this method works. First, we shall study the adsorption of hydrogen on platinum in greater detail, and then we shall use a simplified method in order to understand the variation in the rate constant for the hydrogen reaction in a series of nanostructures of Pd deposited on Au(111).

### The adsorption of hydrogen on Pt(111)

The theory that we want to apply rests on two model Hamiltonians proposed by one of us [13] and by Santos, Koper, and Schmickler [14]. It incorporates elements of the theories of Marcus [7] and of the Anderson–Newns model [18, 19] and provides a framework both for simple and for bond-breaking electron transfer.

We shall present only those elements that are needed for the particularly simple case of proton adsorption on a bare platinum surface. Thus, the process that we consider corresponds to what is often called the underpotential deposition of hydrogen, since it sets in at potentials above the equilibrium potential for the hydrogen electrode.

When a hydrogen atom, or a proton, is close to the surface of a metal electrode, its orbitals are modified by the interaction with the metal. They are broadened and acquire a width  $\Delta(\epsilon)$  and are shifted by an amount  $\Lambda(\epsilon)$ . In general, both  $\Delta$  and  $\Lambda$ , which are also known as the chemisorption functions, may depend on the electronic energy  $\epsilon$ , a point to which we shall return below. In addition, the reactant interacts with the solvent; the strength of this interaction is characterized by the energy of reorganization  $\lambda$ . Thereby, the energy of the orbital depends on the configuration of the solvent, which is described by the solvent coordinate  $q$ , which has the following meaning: When the solvent is in a configuration  $q$ , it would be in equilibrium with a reactant of charge  $-q$ . Thus, during the adsorption of a proton, the solvent coordinate passes from  $q = -1$  to  $q = 0$ . Taking both the interaction with the electrode and with the solvent into account, the density of states (DOS) of the 1-s orbital of hydrogen takes the form:

$$\rho_a(\epsilon) = \frac{1}{\pi} \frac{\Delta(\epsilon)}{[\epsilon - (\epsilon_a + \Lambda(\epsilon) - 2\lambda q)]^2 + \Delta(\epsilon)^2} \quad (1)$$

In the simplest case, in which  $\Delta(\epsilon)$  and  $\Lambda(\epsilon)$  are constant, the DOS of the reactant has the form of a Lorentz distribution, whose center depends on the configuration of the solvent. The occupation of the orbital is obtained by integrating the DOS up to the Fermi level, which we take as our energy zero:

$$\langle n_a \rangle = \int_{-\infty}^0 \rho_a(\epsilon) d\epsilon \quad (2)$$

where the Fermi–Dirac distribution has been approximated by a step function.

Solvent fluctuations can lift the center of the 1-s orbital of hydrogen above the Fermi level, so that it is empty and its state corresponds to a solvated proton, or it can push it below the Fermi level, so that it is filled and the particle is better described as an adsorbed hydrogen atom. The energy of solvation of the proton is particularly large—of the order of 11–12 eV—and the energy of reorganization must be a sizable fraction of this, perhaps about a quarter [21]. Therefore, the energy of activation required for such a solvent fluctuation is very high in the absence of a good catalyst. This is the reason why hydrogen evolution requires such a

high overpotential on bad catalysts like mercury and cadmium.

In order to perform calculations for specific systems, and to understand their catalytic behavior, we need to calculate the chemisorption functions. These depend on the band structure of the metal and on the interaction with the reactant. Metals that are used as electrode materials have two kinds of bands near the Fermi level: an *sp* band, which is generally broad and extends well across the Fermi level, and a *d* band, which is narrower, has more structure, and whose position varies widely between different types of metal. Consequently, the energy broadening  $\Delta$  has two contributions, one from each band. The part  $\Delta_{sp}$  pertaining to the *sp* band can be taken as independent of the energy, since this band has little structure near the Fermi level. In contrast, the part pertaining to the *d* band depends on the structure of that band. To a good approximation, it is proportional to the DOS of the metal *d* band:

$$\Delta_d(\epsilon) = |V|^2 \pi \rho_d(\epsilon) \quad (3)$$

where  $V$  is the coupling constant between the reactant and the *d* band. The other function, the level shift  $\Lambda$ , is obtained from  $\Delta$  through a transform:

$$\Lambda(\epsilon) = \frac{1}{\pi} \mathcal{P} \int_{-\infty}^{\infty} \frac{\Delta(\epsilon')}{\epsilon - \epsilon'} d\epsilon' \quad (4)$$

where  $\mathcal{P}$  denotes the principal part. Therefore, in order to calculate the effect of the *d* band on the reaction, we need the DOS of the *d* band, which is easily obtained from DFT, and the coupling constant; we indicate below how to obtain the latter from DFT as well. The technical details of all the DFT calculations performed are given in the [Appendix](#).

When the DOS of the reactant is known, the electronic energy, as a function of the solvent coordinate  $q$ , is obtained by integrating over the occupied part:

$$E_e = \int_{-\infty}^0 \epsilon \rho_a(\epsilon) d\epsilon \quad (5)$$

To this, we must add the energy of the solvent; its interaction with the electron on the hydrogen has already been accounted for in the DOS. Therefore, we only need to add the energy in the absence of interactions and the interaction with the positive charge on the proton:

$$E_{sol} = \lambda q^2 + 2\lambda q \quad (6)$$

It is easy to verify that this energy attains its minimum value of  $-\lambda$  at  $q = -1$ , which is the solvent configuration that corresponds to the proton.

To a first approximation, the total energy is the sum of the electronic energy calculated from Eq. 5

and the solvent energy, and this is good enough to establish trends in hydrogen catalysis [21]. However, for quantitative calculations, we have to go beyond the one-electron model and include the exchange and correlation interaction of the electron on the hydrogen atom with the metal. For this purpose, we perform DFT calculations for the hydrogen atom adsorbed on Pt(111). This is completely discharged, and its energy corresponds to a solvent coordinate of  $q = 0$ . We calculate the electronic energy for the same configuration from Eq. 5; the difference  $\Delta E$  between the two results is the exchange and correlation part that was missing. In order to obtain this correction for arbitrary values of  $q$ , we assume that it is proportional to the occupation of the hydrogen orbital:

$$\Delta E(q) = \Delta E(q = 0) \times \langle n_a \rangle \quad (7)$$

This equation is obviously correct in the limits when  $\langle n_a \rangle = 1$  and  $\langle n_a \rangle = 0$ , and the linear interpolation is natural. Of course, this is an approximation, but DFT itself is based on approximations of this kind, and there is no reason why this approximation should be worse than the others.

In order to calculate the free energy surface for the adsorption of hydrogen, we proceed as follows. The equilibrium position is known to be the fcc hollow site; we calculate the adsorption energy of the atom for the equilibrium distance, at about 0.89 Å, and for a series of positions vertically above this site but at larger distances. For separations larger than about 2.4 Å spin polarization sets in [22];<sup>1</sup> however, for the distances that we need, we can ignore spin. For each distance, we also calculate the DOS projected onto the 1-s orbital of hydrogen, which we fit to the model DOS of Eq. 1, taken at  $q = 0$ , by choosing the three unknown parameters:  $|V|^2$ ,  $\epsilon_a$ , and the broadening  $\Delta_{sp}$  caused by the  $sp$  band. An example is shown in Fig. 1; it corresponds to a distance of 1.2 Å. The fitted parameters in this case are:  $|V|^2 = 2.29 \text{ eV}^2$ ,  $\epsilon_a = -5.72 \text{ eV}$ , and  $\Delta_{sp} = 0.69 \text{ eV}$ . The center of the hydrogen 1-s orbital lies somewhat below the  $d$  band of platinum, but its DOS overlaps with this band.

At this stage, we note in passing that not all authors agree that the fcc hollow site is the favored site for adsorption. Ishikawa et al. [20], using different functionals, have found the bridge site to be more favorable. In fact, the adsorption energies on the principle sites—hollow, bridge, on top—are quite similar, so that

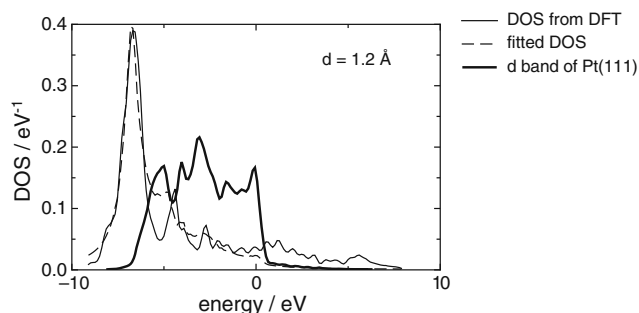


**Fig. 1** Density of states of the 1-s orbital when the H atom is at a distance of 1.2 Å in front of the surface, both calculated by DFT and fitted according to Eq. 1. The  $d$  band DOS of Pt(111) is also shown

different versions of DFT may give different results, though the majority of authors favor the fcc hollow site. Our method would work just as well if another site was favored.

As mentioned above, the part that is least understood is the reorganization of the solvent. In previous publications, it has been estimated as  $\lambda \approx 3 \text{ eV}$  [21, 23], and for calculations that do not explicitly consider the distance dependence, it is sufficient to use a constant value. However, when the hydrogen atom is right at the surface,  $\lambda$  is certainly smaller than when it is in its final state, in which, according to computer simulations, it is part of a Zundel ion [10, 24]. We therefore follow previous suggestions that, right at the surface,  $\lambda$  is lower by a factor of two [25]. Fortunately, the value near the surface is not really important, because there, the hydrogen is almost completely discharged, and its interaction with the solvent practically vanishes. Also, as we shall see below, the value of  $\lambda$  is partially canceled by another term.

This other term contains the interactions of the proton in the final state, which have not yet been considered. So far, the energy of the proton would be just  $-\lambda$ , but this is only the interaction with the slow solvent modes. The parts that are missing are the interactions with the fast solvent modes, the image force, and the interaction with the electrostatic potential. Fortunately, we do not have to consider them explicitly since we know that, at the equilibrium potential, the free energy of the proton must be one half of the free energy  $E_i$  of the hydrogen molecule. Therefore, we write:

$$V_f = (1 - \langle n_a \rangle)(E_i/2 + \lambda - e_0\eta), \quad (8)$$

where the interaction has been assumed to be proportional to the charge. The last term accounts for the effect of an overpotential  $\eta$ . The energy of the  $\text{H}_2$

<sup>1</sup>For the case of hydrogen on Cu(111), this was shown by [22]. According to our own calculations, at Pt(111), it sets in at about the same distance.

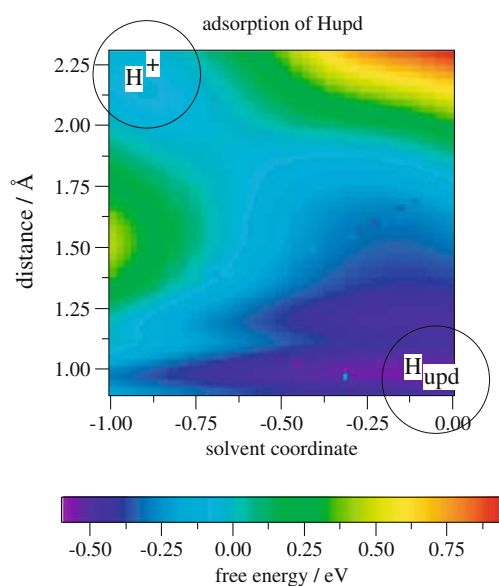


**Fig. 2** Free energy surface for the adsorption of  $H_{\text{upd}}$  on Pt(111)

molecule is  $-31.73$  eV, and the entropic contribution is  $-0.41$  eV [5], which gives:  $E_i = -32.11$  eV.

With these preparations, we can now present the free energy surface for the adsorption of hydrogen upd on Pt(111); the result is shown in Fig. 2 for the equilibrium potential. The adsorbed state has an energy that is about 0.2 eV lower than that of the solvated proton. The energy of activation, which is the saddle point on this surface, is practically zero, i.e., lower than 0.1 eV. Thus, in accordance with experimental data, our calculations indicate that the adsorption starts at

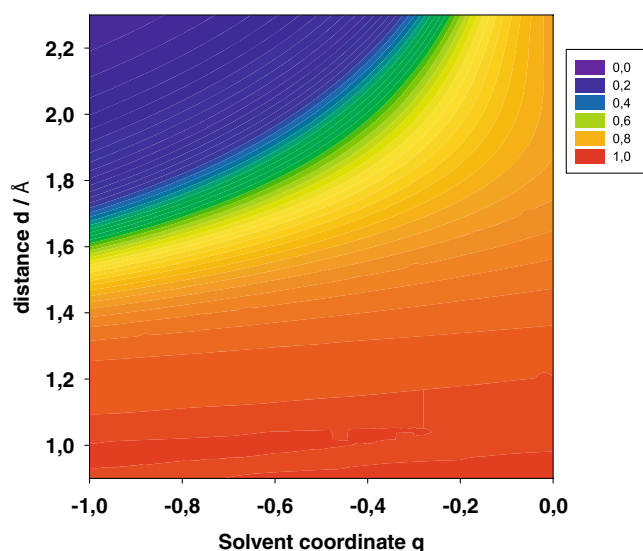


**Fig. 3** Occupancy of the hydrogen 1-s orbital during the adsorption on Pt(111)

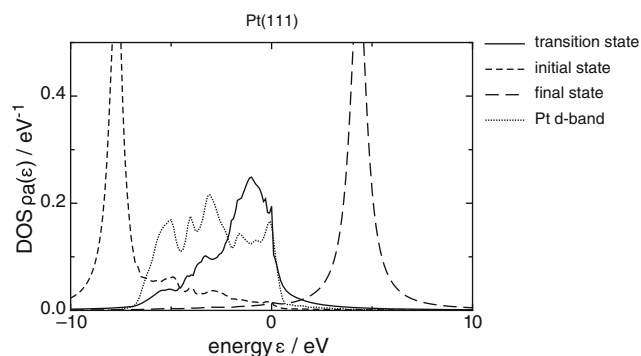


**Fig. 4** DOS of the hydrogen 1-s orbital for the adsorbed atom (full line, left), the proton (long dashes, right), and at the transition state (short thick dashes, center). The  $d$  band of Pt(111) is also shown

potentials above the equilibrium potential, and that the reaction rate is very fast. It is also in line with previous results based on a simplified, one-dimensional potential energy curve [23]. We note in passing that, in the latter publication, we have shown that our model predicts an energy of activation of about 0.5 eV for the Volmer reaction on Au(111) and more than 1 eV for Cd(0001), thus explaining the large difference in the catalytic activity between these metals.

Figure 3 shows how the occupancy of the hydrogen 1-s orbital changes during the reaction, starting from  $\langle n_a \rangle = 0$  for the proton (upper left corner) and reaching unity in the adsorbed state (lower right corner). On the reaction path, the DOS of the hydrogen 1-s orbital changes substantially (see Fig. 4). For the proton, it lies high above the Fermi level and is, therefore, empty. In the adsorbed state, it lies beneath the platinum  $d$  band (see also Fig. 1) and is completely filled. At the transition point, it is greatly broadened by the strong interaction with the  $d$  band. As we have explained in detail in previous publications [16, 17, 23], it is this broadening of the DOS at the saddle point that lowers the energy of activation and affects catalysis. This broadening is particularly strong on Pt, and hence, it is such a good catalyst for the hydrogen reaction.

### Hydrogen oxidation on Pd/Au(111)

The electrocatalytic properties of an electrode depend not only on the composition, but also on the structure. It is well known that nanostructured materials show different activities than bulk materials. This nano-sized effect has been attributed to changes in electronic properties. An interesting case is Au(111) modified by adsorbed layers of palladium. Experimental results



show that the rate of hydrogen evolution increases with decreasing numbers of Pd layers on Au(111), and it is considerably higher for submonolayers; i.e., the fewer Pd islands there are on the surface, the higher is the catalytic activity [28, 29]. Qualitative explanations based on the position of the *d*-bands center have been proposed by the authors. However, there is a lack of theoretical foundation to explain these observations, and the phenomenon remains not well understood.

A full treatment of the various structures using the formalism outlined in the previous section would require very extensive DFT calculations for the various structures. Instead, we shall use a simpler version, with which we have previously explained the trends in the rate of hydrogen reaction on various metals [21]. Instead of performing DFT calculations for many positions of the H<sub>2</sub> molecule and the H atom over the various substrates, we follow our previous work [26] and use the Hückel theory to describe the bonding of the molecule and use DFT only to obtain the *d* band structures of the substrates.

For the hydrogen molecule, we have to consider two orbitals, the 1σ bonding and antibonding orbitals. Also, it is mandatory to consider spin explicitly since, in the isolated molecule, the bonding orbital is occupied by two electrons with opposite spin. The DOS of the

molecule therefore contains two terms and takes the form:

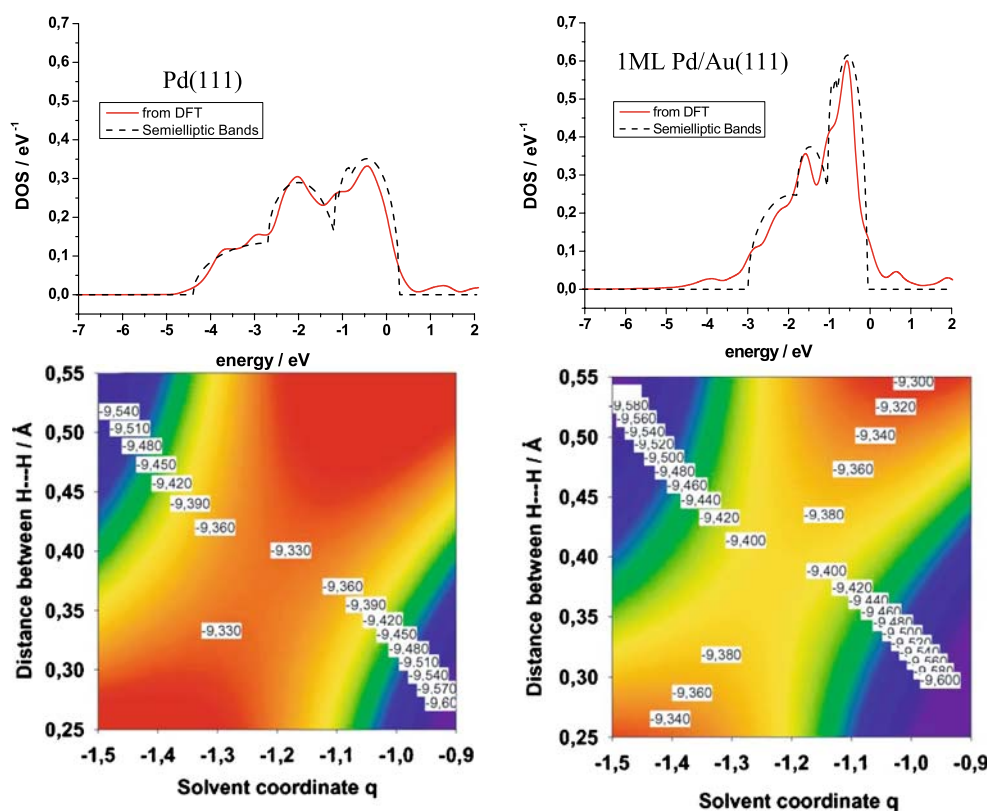
$$\rho_a = \frac{1}{\pi} \sum_{\sigma} \left\{ \frac{\Delta(\epsilon)}{(\epsilon - \tilde{\epsilon}_{\sigma} - \beta)^2 + \Delta(\epsilon)^2} + \frac{\Delta(\epsilon)}{(\epsilon - \tilde{\epsilon}_{\sigma} + \beta)^2 + \Delta(\epsilon)^2} \right\} \quad (9)$$

Here,  $\beta$  is the Hückel binding constant; it is taken as positive and its value is obtained from the binding energy of the hydrogen molecule (4.54 eV). The first term is the DOS for the bonding, the second for the antibonding orbital, and the sum is over the two spin states  $\sigma = \pm 1$ .

The effective energy level  $\tilde{\epsilon}_{\sigma}$  contains the interaction with the solvent and the level shift  $\Lambda(\epsilon)$ , which have been given explicitly in Eq. 1, and also the following terms: the repulsion between different spin states, governed by the Coulomb repulsion  $U$ , the orbital overlap  $S$ , and a small dipole–dipole repulsion term, which becomes effective when the two hydrogen atoms carry charge—the dipoles are formed by the charge and the image charge on the metal. Explicitly, we have:

$$\tilde{\epsilon}_{\sigma} = \epsilon_a - 2\lambda q + \Lambda(\epsilon) + S\beta + U\langle n_{-\sigma} \rangle - \gamma(1 - \langle n_{\sigma} \rangle + \langle n_{-\sigma} \rangle), \quad (10)$$

**Fig. 5** Upper part: density of states (DOS) corresponding to the *d*-bands of Pd obtained from DFT calculations (full lines) and fitted with three semielliptic functions (dashed lines) for the surface orientation (111) of six layers of Pd (left) and five layers of Au with a deposit of a monolayer of Pd (right). Bottom part: contour plots of potential energy surfaces showing the saddle point of the reaction path for the hydrogen oxidation. The projections are done on the plane of the solvent coordinate  $q$  and the distance between both hydrogen atoms relative to the equilibrium in the molecule

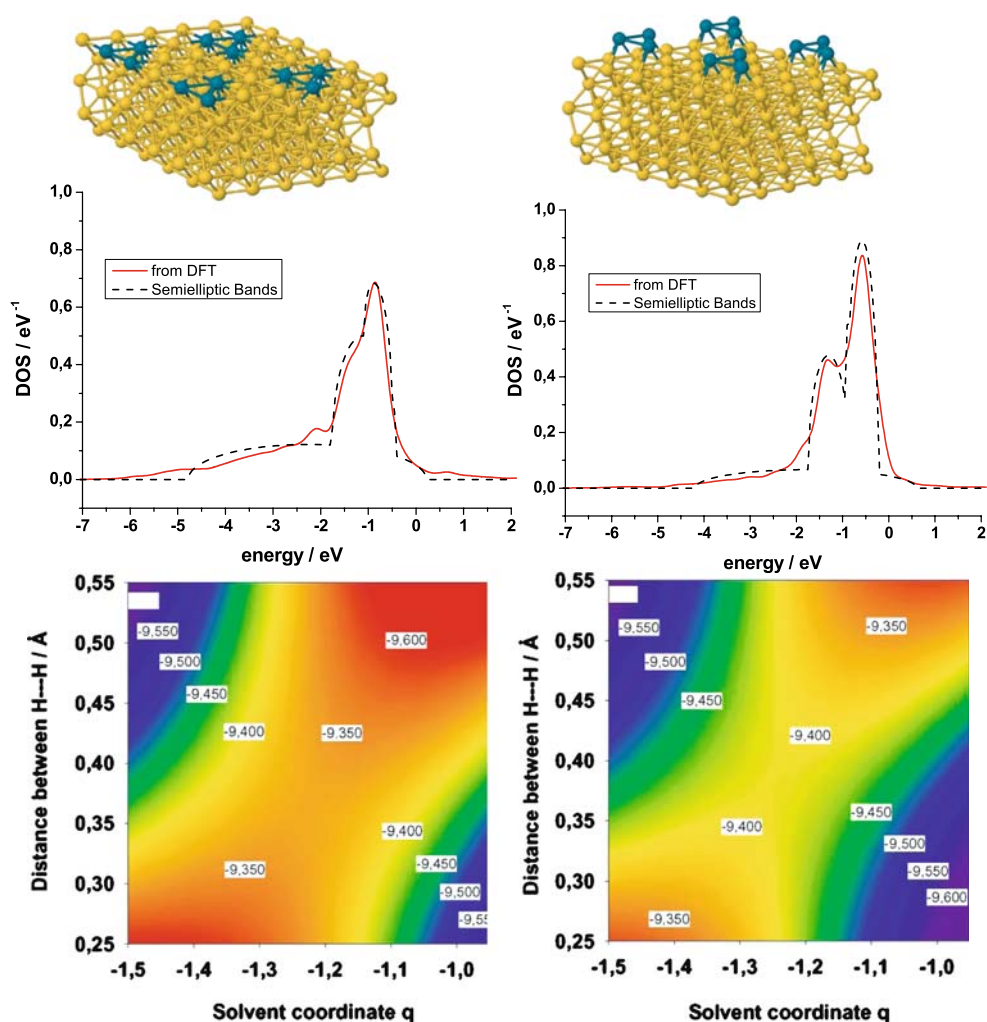


where the last term is the dipole–dipole term. Generally, we have used the same parameters as in [21]:  $U = 4$  eV, and for the overlap  $S$ , we again used the Wolfsberg–Helmholtz approximation; only for the solvent reorganization, we have used the value of  $\lambda = 3$  eV in accordance with the value used in the previous section. As before, the system is not spin-polarized. The value of  $\epsilon_a$  depends on the electrode potential; it was chosen such that the reaction is in equilibrium.

The purpose of our calculation is to explain the variation of the rate with the structure of the substrate. For this purpose, we have obtained the band structures of the systems from DFT calculations. These data were then fitted with a set of three semielliptical functions in order to have analytical expressions for the chemisorption functions  $\Delta(\epsilon)$  and  $\Lambda(\epsilon)$  given by Eqs. 3 and 4. The coupling constant was set to  $|V|^2 = 6.3$  eV<sup>2</sup>, the value recommended by Hammer and Nørskov [30] for the interaction of hydrogen with a Pd(111) surface, and has been employed for all configurations of Pd on Au(111).

Figure 5 shows the results obtained for a bare Pd(111) surface in comparison with those for a monolayer of Pd deposited on a Au(111) surface. The DOS of the  $d$  bands change markedly. For the monolayer of Pd, they are shifted to more positive energies compared to bulk Pd, and the bands become thinner, indicating a stronger localization of the electrons. The lattice constants for bulk Pd and Au are 3.96 and 4.18 Å, respectively. The misfit between the lattice constants of Au and Pd induces a strain in the overlayer, which also changes the electronic properties. The monolayer of Pd is expanded relative to the surface of the bulk material, facilitating the localization. These changes in the electronic structure produce an increase of the electrocatalytic properties for the hydrogen oxidation, even if the coupling constant  $|V|^2$  remains unchanged. This effect is clearly observed in the contour plot of the potential energy surfaces shown in the figure for both systems. The coordinates for these surfaces are the distance between both hydrogen atoms relative

**Fig. 6** Submonolayer of Pd on Au(111) with a coverage degree of 0.33 for two different distributions of the Pd: cluster of three atoms embedded in the surface of Au(111) replacing Au atoms in the lattice (*left*) or deposited as overlayer on the hollow sites of the Au(111) surfaces (*right*). *Upper part*: unit cells employed for the DFT calculations. *Middle part*: Density of states (DOS) corresponding to the  $d$  bands of Pd obtained from DFT calculations (*full lines*) and fitted with three semielliptic functions (*dashed lines*). *Bottom part*: contour plots of potential energy surfaces showing the saddle point of the reaction path for the hydrogen oxidation. The projections are done on the plane of the solvent coordinate  $q$  and the distance between both hydrogen atoms relative to the equilibrium in the molecule



to the equilibrium position in the molecule and the normalized solvent coordinate  $q$ . The important region is the saddle point, where the electronic transition takes place. An energy decrease of the barrier of about 0.07 eV is observed, which means about an order of magnitude in the rate constant at room temperature.

Other authors have explained the increase of the rate with the fact that the energy of adsorption of hydrogen on the Pd overlayer is lower than on bulk Pd(111) [31, 32]. However, since hydrogen is already strongly adsorbed on Pd(111), a mere lowering of the adsorption energy would seem to inhibit the reaction rather than catalyze it.

The other example we have analyzed is a submonolayer of Pd on Au (111), with a coverage degree of 0.33. Two different distributions of the Pd atoms have been considered: a cluster of three atoms embedded in the surface of Au(111), replacing Au atoms in the lattice, or deposited as an overlayer on the hollow sites of the Au(111) surfaces. Also in this case, important changes are observed in both the DOS of the  $d$  bands of Pd and in the electrocatalytic properties. It is evident from the contour plots of the energy surfaces shown in Fig. 6 that the overlayer of Pd is more favorable for the oxidation of hydrogen, where the reaction occurs about seven times faster.

The two examples shown here are in line with the experimental results presented in [28, 29]. It is satisfying that, even in a simplified model for the interactions between the hydrogen atoms, such as the Hückel method, the calculations lead to the right experimental trend. Obviously, a more detailed treatment is necessary to get quantitative results and provide further details about the mechanism of the hydrogen oxidation reaction. However, the present results show that the role of the interactions of the molecule with the electrocatalyst in the electrochemical environment including solvent effects and potential are crucial to explain the different activities of different materials and surface structures.

**Acknowledgements** Financial support by the Deutsche Forschungsgemeinschaft (Schm 344/34-1 and Sa 1770/1-1), and of the European Union under COST is gratefully acknowledged. E. S. thanks CONICET for continued support. A.L. gratefully acknowledges a postdoctoral fellowship of the Swedish Research Council.

## Appendix: Details of DFT calculations

All calculations were performed using the DACAPO code [33]. This utilizes an iterative scheme to solve the Kohn–Sham equations of DFT self-consistently. A plane-wave basis set is used to expand the electronic

wave functions, and the electron–ion interactions are accounted through ultrasoft pseudopotentials [34], which allows the use of a low-energy cutoff for the plane-wave basis set. An energy cutoff of 400 eV, dictated by the pseudopotential of each metal, was used in all calculations. The electron–electron exchange and correlation interactions are treated with the generalized gradient approximation in the version of Perdew, Burke, and Ernzerhof [35]. The Brillouin zone integration was performed using a  $16 \times 16 \times 1$   $\mathbf{k}$ -point Monkhorst–Pack grid [36] corresponding to the  $(1 \times 1)$  surface unit cell. The surfaces were modeled by a  $(3 \times 3)$  supercell with four metal layers and six layers of vacuum. Dipole correction was used to avoid slab–slab interactions [37]. The first two top layers were allowed to relax, while the bottom two layers were fixed at the calculated next neighbor distance (Au: 2.95 Å, Pd: 2.82 Å, Pt: 2.83 Å). The optimized surfaces (prerelaxed) in the absence of the hydrogen atom were used as input data to carry out the calculations to study the hydrogen desorption. For each system, we performed a series of calculations for a single atom adsorbed on a fcc hollow site and varied its separation from the surface. The prerelaxed surface was kept fixed while the H was allowed to relax in  $xy$  coordinates during these calculations. At each position, we calculated the adsorption energy and the DOS projected onto the 1-s orbital of hydrogen, and from the latter, we obtained the model DOS of Eq. 1 by fitting.

## References

1. Tafel J (1905) *Z Phys Chem* 50:641
2. Erdey-Gruz T, Volmer M (1930) *Z Phys Chem A* 150:203
3. Trasatti S (1972) *J Electroanal Chem* 39:163
4. Trasatti S (1977) *Adv Electrochem Electrochem Eng* 10:213
5. Nørskov JK, Bligaard T, Logadottir A, Kitchin JR, Chen JG, Pandelov S, Stimming U (2005) *J Electrochem Soc* 152:J23 (1985) 138.
6. Conway BE, Beatty EM, DeMaine PAD (1962) *Electrochim Acta* 7:39
7. Marcus RA (1956) *J Chem Phys* 24:966
8. Hush NS (1958) *J Chem Phys* 28:962
9. Levich VG (1970) Kinetics of reactions with charge transfer. In: Eyring H, Henderson D, Jost W (eds) *Physical chemistry, and advanced treatise*, vol Xb. Academic, New York
10. Otani M, Hamada I, Sugino O, Morikawa Y, Okamoto Y, Ikeshoji T (2008) *Phys Chem Chem Phys* 10:3609
11. Skulason E, Karlberg GS, Rossmeisl J, Bligaard T, Greeley J, Jonsson H, Nørskov JK (2007) *Phys Chem Chem Phys* 9:3241
12. Otani M, Hamada I, Sugino O, Morikawa Y, Okamoto Y, Ikeshoji T (2008) *J Phys Soc Jpn* 77:024802
13. Schmickler W (1986) *J Electroanal Chem* 204:31
14. Santos E, Koper MTM, Schmickler W (2006) *Chem Phys Lett* 419:421
15. Santos E, Koper MTM, Schmickler W (2008) *Chem Phys* 344:195
16. Santos E, Schmickler W (2006) *Chem Phys Chem* 7:2282



17. Santos E, Schmickler W (2007) *Chem Phys* 332:39
18. Anderson PW (1961) *Phys Rev* 124:41
19. News DM (1969) *Phys Rev* 178:1123
20. Ishikawa Y, Mateo JJ, Tryk DA, Cabrera CR (2007) *J Electroanal Chem* 607:37
21. Santos E, Schmickler W (2007) *Angew Chem Int Ed* 46: 8262
22. Mizielinki MS, Bird DM, Persson M, Holloway S (2005) *J Chem Phys* 22:084710
23. Santos E, Pötting K, Schmickler W (2008) *Discuss Faraday Soc* (in press)
24. Wilhelm F, Schmickler W, Nazmutdinov RR, Spohr E (2008) *J Phys Chem C* 112:10814
25. Schmickler W (1995) *Chem Phys Lett* 237:152
26. Santos E, Schmickler W (2008) *Electrochim Acta* 43x:6149
27. Karlsberg GS, Jaramillo TF, Skulason E, Rossmeisl J, Bligaard T, Nørskov JK (2007) *Phys Rev Lett* 99:126101
28. Pandelov S, Stimming U (2007) *Electrochim Acta* 52:5548
29. Kibler LA (2006) *Chem Phys Chem* 7:985
30. Hammer B, Nørskov JK (2000) *Adv Cat* 45:71
31. Meier J, Schiøtz J, Liu P, Nørskov JK, Stimming U (2004) *Chem Phys Lett* 90:440
32. Roudgar A, Groß A (2004) *Surf Sci* 559:L180
33. Hammer B, Hansen LB, Nørskov K (1999) *Phys Rev B* 59:7413. <http://www.fysik.dtu.dk/campos>
34. Vanderbilt D (1990) *Phys Rev B* 41:7892
35. Perdew JP, Burke K, Ernzerhof M (1996) *Phys Rev Lett* 77:3865
36. Monkhorst HJ, Pack JD (1976) *Phys Rev B* 13:5188
37. Bengtsson L (1999) *Phys Rev B* 59:12301